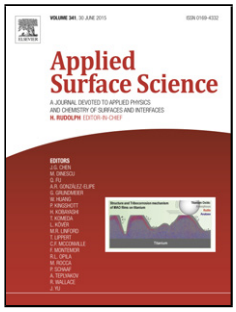

Title: Surface Analysis of 316 Stainless Steel Treated with Cold Atmospheric Plasma

Authors: David F. Williams, Ewen J.C. Kellar, David A. Jesson, John F. Watts

PII: S0169-4332(17)30162-9
DOI: http://dx.doi.org/doi:10.1016/j.apsusc.2017.01.150
Reference: APSUSC 34945

To appear in: *APSUSC*

Received date: 7-12-2016
Revised date: 10-1-2017
Accepted date: 16-1-2017

Please cite this article as: David F.Williams, Ewen J.C.Kellar, David A.Jesson, John F.Watts, Surface Analysis of 316 Stainless Steel Treated with Cold Atmospheric Plasma, Applied Surface Science http://dx.doi.org/10.1016/j.apsusc.2017.01.150

Surface Analysis of 316 Stainless Steel Treated with Cold Atmospheric Plasma

David F Williams*[1, 2], Ewen J C Kellar[2], David A Jesson[1], John F Watts[1]

[1]Department of Mechanical Engineering Sciences

UNIVERSITY OF SURREY

Guildford Surrey GU2 7XH UK

[2]TWI Ltd Granta Park Great Abington

Cambridge CB21 6AL UK

Corresponding Author* - david.williams@surrey.ac.uk

Graphical abstract

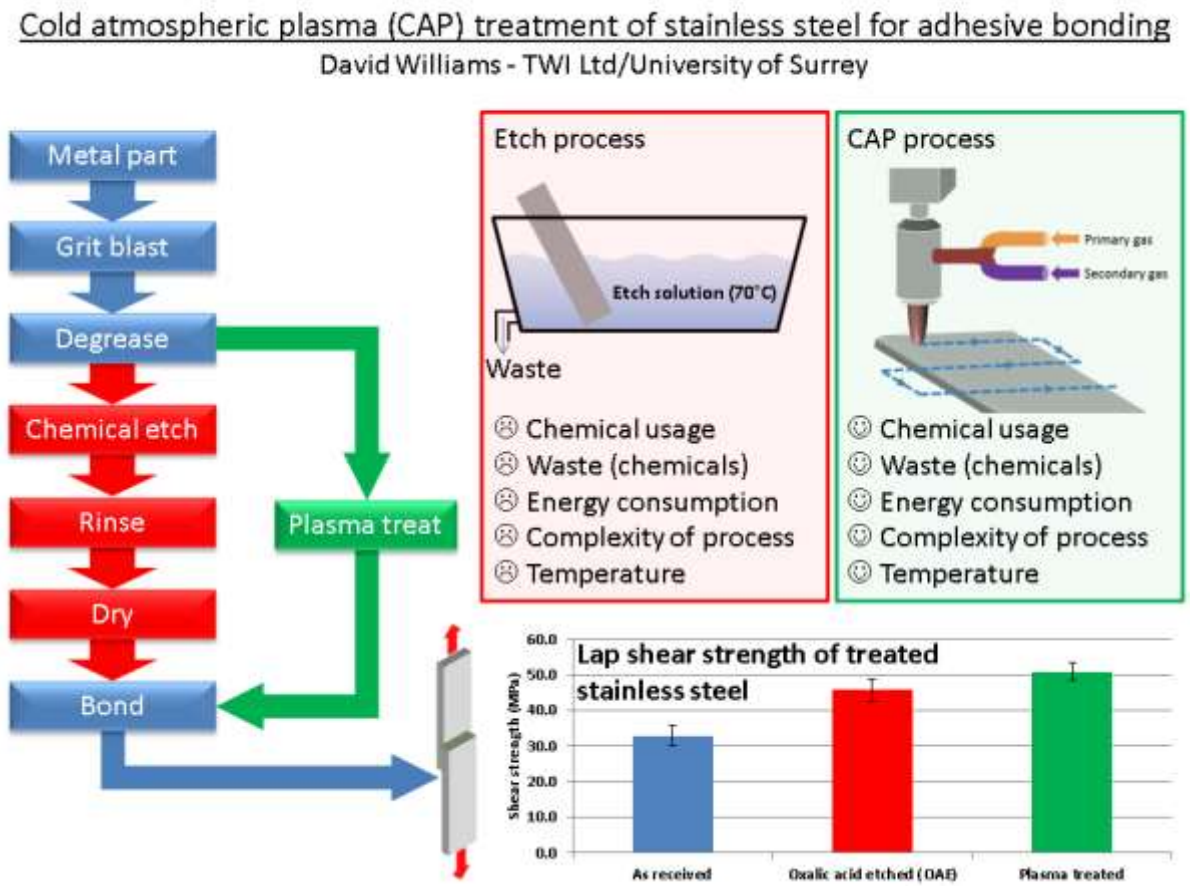

Highlights

- Reduction in carbon contamination from ~80 at.% to 40 at.% after 15 second treatment.
- Associated carbon thickness reduction from 4.5 nm to 0.5 nm
- Area treated by torch has a diameter of 11 mm measured using imaging XPS.

Abstract

The surface of 316 stainless steel has been modified using cold atmospheric plasma (CAP) to increase the surface free energy (by cleaning the and chemically activating the surface)IN preparation for subsequent processes such as painting, coating or adhesive bonding. The analyses carried out, on CAP treated 316 stainless steel surfaces, includes X-ray photoelectron spectroscopy (XPS), imaging XPS (iXPS), and surface free energy (SFE) analysis using contact angle measurements.

The CAP treatment is shown to increase the SFE of as-received 316 stainless steel from ~39 mJ m^{-1} to >72 mJ m^{-1} after a short exposure to the plasma torch. This was found to correlate to a reduction in adventitious carbon, as determined by XPS analysis of the surface. The reduction from ~90 at% to ~30% and ~39 at%, after being plasma treated for 5 minutes and 15 seconds respectively, shows that the process is relatively quick at changing the surface. It is suggested that the mechanism that causes the increase in surface free energy is chain scission of the hydrocarbon contamination triggered by free electrons in the plasma plume followed by chemical functionalisation of the metal oxide surface and some of the remaining carbon contamination layer.

Keywords: Contact angle, iXPS, Surface Modification, XPS

1 Introduction

1.1 Pre-Treatment Methods

The surface of a material is a critical feature to consider with regards to how it will interact with the surrounding environment. Beyond the bulk properties (*e.g.* strength, toughness), which are the usual focus during material selection, the surface properties can influence how the material can be joined, painted or functionalised, or indeed how it reacts to aggressive environments *i.e.* corrosion resistance, oxidation resistance and the like. These are important aspects to consider during material selection as it can affect structural integrity and, potentially, the durability of any adhesive joint that is fabricated or coating that is applied.

The surface properties of a material can be modified by using different processes, which can be mechanical, energetic, chemical or a combination of these approaches each of these have its own advantages and disadvantages [1].

Mechanical processes

Mechanical processes such as grit blasting or abrasion generally act to increase the rugosity of the surface, and they are relatively material independent processes. This increases the surface area which can be beneficial for joining and painting, if the roughness is on a micrometre scale. There is also material removal, normally some or all of the surface oxide (in the case of metals) which will reduce surface contamination

but these processes also have the potential to leave contamination behind, in the form of embedded particles for example, and therefore sometimes require supplementary cleaning steps prior to further processing. Additionally, there is the danger that such adventitious material may be redeposited if abrasive media, (grit, wire brush bristles etc) is reused. These processing methods are simplistic they are often effective in terms of enabling high initial bond strength and the equipment can beautomated and/or mounted on robots. However, there are issues around controlling the process. While the equipment can be mounted on robots there is difficulty in quantifying the grit-blasted surface: visual inspection is a common approach, but this adds to the cost and slows down the processing of a surface [2].

Chemical processes

Chemical pre-treatment processes can produce many different surface topographies and chemistries. Examples include chemical etching and anodising the variety in terms of the chemistry used is vast and further information can be found in other published work [3–6]. These processes leave surfaces that are rough at both the micrometre and nanometre scale with excellent wetting properties and have the potential to produce a strong bond with the adhesive or paint. Chemical processes are widely used in industry because of the excellent and diverse properties of the surface finish that are possible. They are usually energy intensive as the chemicals required take a large amount of processing during manufacture and disposal [7] and are also generally used at elevated temperature (typically75-85°C).

These processes are generally wet (aqueous-based) which means that treating complex shapes is easily possible but the parts have to be dried and have residue removed before further processing often washing and further drying [8]. Chemical treatments tend to be tailored to a specific metal which leads to a situation whereby each materials requires its own chemical treatment; in turn this makes the manufacture of multi material structures more complex.

Energetic Processes

Energetic processes such as flame, laser and plasma treatments are dry systems that can alter, etch or chemically functionalise the surface [9]. Laser modification at sufficiently high power can melt the surface of the substrate, be it ceramic, metal or polymer, and ablate it to produce a roughening effect. This can be beneficial but

requires a large amount of energy, and local melting of the surface can lead to changes in the bulk properties as a result of microstructural changes [10], it is however, known to be an efficient method of treating polymers and ceramics for adhesive bonding [11,12].

Plasma Treatment

Plasma treatment has been used for many years to treat polymers prior to painting, printing or bonding. The plasma treatment for polymers can be divided into corona /dielectric barrier discharge (DBD), flame treatment and low pressure plasma treatment. Probably the most widely used is either corona or DBD. These can be considered atmospheric plasmas as they operate at ambient pressure in atmosphere. Their methods of generation are discussed in detail by Conrads [13]. Most polymers react well to such treatments as they have a favourable structure to modify, and it is readily straightforward to increase the surface free energy to a level necessary for bonding and other adhesion phenomena. These plasma sources are well suited to polymer applications as they can be placed in a production line close to the polymer web being treated on a roll: this is carried out in air and known as corona treatment [14]. As the plasma is only effective over a small distance this can be easily controlled using simple geometries: using corona on a complex 3D structure however is not possible, but flame treatment used in conjunction with robotic positioning of the flame head is viable [9], as is the use of robots to position a plasma torch. Low pressure plasma treatment is essentially a batch process that is still widely used for high added-value components despite the increased cost and time for treatment.

The plasma treatment of metals is much less widespread. There are some applications which use low pressure plasma to modify the surface of components prior to painting or bonding but these are batch processes which lend themselves to low volume production and manufacturing [15–17].

Cold atmospheric plasma is a method of plasma generation which has not been as thoroughly investigated as other methods of treating surfaces. It was developed and is being used for the pre-treatment of polyolefins *e.g.* [18–20], and has since been applied to the surface modification of metals, this has been investigated to a lesser extent compared to polyolefin treatment and the current analysis of the plasma treated of metals is limited to surface topography, surface free energy and single spot XPS analysis, which are invariably area integrating analyses of several to many square millimetres in area. While these do elucidate to the level of treatment at the centre of the treated area there is little work that has been done to probe the area surrounding

the treated area. This is an important aspect of the treatment to consider as this will enable the use of multiple passes using one torch to treat a large area [21–23].

This work looks to complete the XPS analysis of a single plasma setup by analysing the entire treated area. This will allow for a more detailed knowledge of how the plasma interacts with the surface. Furthermore it will allow for the start of a comparison of different nozzle parameters and how changing the nozzle diameter, for example, could change the size of the treated area as there are applications where using a sub millimetre plasma torch may be advantageous such as micro-electronics [24]

This paper describes work conducted using a variant of a cold atmospheric plasma (CAP) treatment, which has been used to treat 316 stainless steel. The chemical and physical properties of surfaces obtained by the CAP treatment of the metal have been studied by calculating the surface free energy change measured using contact angle and X-ray photoelectron spectroscopy (XPS) these have been included to allow for direct comparison between this and other published work. To demonstrate how the plasma changes the area surrounding the centrepoint imaging XPS has been used which is described in Section 2.3.2.

2 Experimental

2.1.1 Steel

AISI 316 stainless steel (SS) purchased from Smiths Metals (Biggleswade, UK) was used for this work. This alloy differs to the more common AISI 304 by the addition of ca. 2 wt% molybdenum which provides improved crevice corrosion resistance. The main uses for the AISI 316 alloy include chemical storage, food processing, marine and surgical applications. The specification for AISI 316 is given in Table 1 along with the composition of the steel used in this project. The material was received with one side linished and covered with a 100 μm thick protective vinyl coating.

The 2 mm thick SS sheet was cut into small coupons using a guillotine. The protective coating was then peeled off the samples, which were acetone wiped with a lint-free cloth prior to CAP treatment. The vinyl coating residue provided a useful control for a steel surface with carbon contamination present (subsequently shown by XPS to be at a thickness of ca. 5 nm) and enabled ready assessment of the efficacy of the CAP treatments studied as a means to remove organic surface contaminants. Samples were treated by CAP as 40 x 40 mm coupons except for the imaging XPS (iXPS) samples which were deliberately larger, 50 x 50 mm, to

avoid missing any of the treated region. Contact angle measurements were made on panels which measured 25 x 100 mm and readings were taken immediately following CAP treatment.

2.2 Plasma

2.2.1 Plasma composition

The plasma torch used in this experiment is a modified Plasma Tact system from Ad-Tec Europe, originally developed for the use of *in vivo* sterilisation of wounds. The base system uses either argon or helium as a feed gas. The modified version used in this research uses argon or helium as a primary gas and has an additional input to allow doping of the inlet gas with other gases. This leads to a number of input gas combinations which are described in Table 2.

The plasma generator is a low power system, with an input requirement of ~150 W to operate and output of 15 W of microwave energy into a small cavity via a central antenna. This ionises the gas allowed into the torch through two high precision mass flow controllers (10 L min^{-1} - primary gas and 5 L min^{-1} - secondary gas). The lines are combined sufficiently far upstream from the torch to ensure that the gas is fully mixed prior to ionisation. As the plasma output power is low, the bulk gas temperature is of the order of 40 - 50 °C at a distance of 15 – 20 mm from the torch.

For this work pure helium gas was used as the input gas. This choice was based on published work [25] showing that it produces a large reduction in carbon contamination when treating metals, accompanied by an increase in surface free energy. For industrial purposes helium may not be an adequate choice as it is an expensive gas to use as a consumable. Future work is planned however using the other gases mentioned in Table 2 to determine if it is possible to produce a comparable surface and therefore be more favourable economically.

The torch is attached to a table with computer controlled 3-axis movement to allow for exact positioning and repeatability with respect to the steel substrate, both in terms of stand-off distance and treatment (torch) speed which can be varied within pre-set limits. Control is managed by Mach3 software, purchased from Artsoft which uses g-code to control the machine coordinates.

There are several differences between cold atmospheric plasma and low pressure plasma. Firstly cold atmospheric plasma operates in ambient conditions compared to a reduced pressure atmosphere used in low pressure plasma. This is advantageous as there is no vacuum equipment needed to operate it but the atmosphere is more controllable when using low pressure plasma. Also, the ionisation ratio of the feed gas is much higher for a low pressure plasma system [26] compared to CAP. This means that there is a greater population

of reactive particles which are present in the plasma compared to atmospheric pressure plasma which may have an effect on the time required to achieve a level of treatment.

Unpublished work carried out at TWI has led to a set of parameters which give the highest, practical, efficacy of treatment judged using surface free energy measurements on an as-received metal substrate. These are presented in Table 3.

2.2.2 Cold Atmospheric Plasma treatment

Initial plasma treatments were conducted for long periods in static mode to ascertain the effect on the steel substrate. This work is then extended to ascertain if the same level of treatment can be achieved with shorter treatments, thus improving treatment efficiency.

Initial trials were conducted with a five-minute exposure time on a single spot. These were then analysed using XPS. It should be noted that less than two minutes elapsed between treatment ceasing and introduction of the specimen into the spectrometer. The analysis was of a spot, of 800µm diameter, at the centre of the treated area.

Subsequent trials were then conducted at 15 seconds dwell time which is a more realistic treatment duration for industrial applications. After a set of high resolution XPS spectra were acquired, iXPS was employed using stage rastering, over an area of serval square centimetres to investigate the distribution of chemical species across the treated area. This has also been used to determine the treatment area achievable with the current torch.

2.3 Analysis

2.3.1 Surface free energy

Surface free energy was calculated using a Kruss DSA 100 with deionised water and diiodomethane as probe fluids. A drop volume of 5 µl and 2 µl respectively was used for the duration of the project, these drop sizes were based on work by Rymuszka [27]. The Fowkes method [28] was used to calculate the polar and dispersive components of the surface free energy. The results are a mean of 5 drops of each probe liquid on the same steel coupon.

Surface free energy calculations have been used to measure the initial efficacy of the treatment. Unpublished work has been done using contact angle measurements to determine the major factors in terms of treatment variables in terms of treatment duration, stand-off distance and gas flow rate.

2.3.2 X-ray photoelectron spectroscopy

Chemical analysis of the substrate pre- and post-treatment was conducted by XPS using a Thermo Scientific Theta Probe, with a Thermo Scientific *Avantage v4.88* datasystem for spectral acquisition and processing, using monochromatic aluminium Kα X-rays. This

technique was used primarily to probe the change in surface chemistry, post treatment. XPS was used in two different modes, spot analysis and iXPS. For iXPS, the instrument was run in snapshot acquisition mode, using a 400 μm diameter X-ray spot with a step size of 400 μm and a pixel array of 64 x 64, each pixel containing a full set of snapshot spectra to be used for quantification and chemical state elucidation. The elemental regions that were acquired using this technique were carbon1s, nitrogen1s, oxygen1s, chromium$2p_{3/2}$ and iron$2p_{3/2}$. This set were chosen as they routinely made up over 95% of the surface in previous analyses and allowed for the acquisition to be made in a timelier manner.

The snapshot method of acquisition relies on the electron dispersion within the analyser to provide a complete spectrum of the core level at the detector at any instant in time, rather than relying on the scanning of the analyser retarding potential, as is the usual mode of operation, and the one used for point analysis in the current work. In the snapshot mode the detector of the electron analyser records electron intensity in each detector channel simultaneously (hence the term snapshot) and consequently a full spectrum is recorded in parallel rather than the usual serial acquisition mode. In snapshot mode the acquisition time is set at a value that ensures a good quality spectrum of the core level of interest. For the Theta Probe spectrometer, the detector consists of 112 channels and the analyser pass energy employed, reflects the binding energy window of the spectrum that is required, the dispersion between inner and outer channels of the detector being of the order of 10% of the pass energy. The pass energies employed to provide appropriate binding energies for the core levels recorded are presented in Table 4. Clearly there is the usual compromise between sensitivity and spectra resolution as a function of pass energy, which in the snapshot mode restricts the width of the spectral window accessible. For this reason, only the iron $2p_{3/2}$ and chromium $2p_{3/2}$ spectra were recorded rather than the more usual 2p doublet of the $2p_{3/2}$ and $2p_{1/2}$. The main reason for using this mode is that the analysis takes 30-45 seconds per element per pixel as opposed to 5-6 minutes. This allows a much larger area to be analysed within a realistic time. The set of spectra at each pixel point were quantified and the variation in transmission resulting from the different pass energies was ameliorated by the inclusion of the appropriate transmission function in the quantification algorithm.

Spot analysis was performed using an X-ray spot size of 800 μm diameter. The usual methodology for this analysis was a survey spectrum with a pass energy of 300 eV, a step size of 0.2 eV and 5 scans followed by a series of high resolution spectra of the core levels of the elements of interest. The high resolution spectra were obtained using a step size of 0.1 eV, pass energies from 30 to 80 eV and between 25 and 100 scans with depending on the concentration of the element.

Using the XPS data, further carbon over-layer thickness values were calculated using the methodology described by Smith [29] who proposed the following equation:

$$d = -\lambda_{C1s,C} cos\theta \ln\left(1 - \frac{x}{100}\right) \qquad \text{Equation 1}$$

Where d is the depth of the carbon over layer in nanometers. $\lambda_{C1s,C}$ is the effective attenuation length of a carbon electron in the hydrocarbon over-layer, circa 3 nm, θ is the electron take off angle, which for the Theta Probe used in this analysis is 56° and x is the quantified carbon concentration in atomic%.

3 Results

3.1 Surface free energy

The results of the surface free energy calculations conducted on 316 SS are presented in Figure 1; the dispersive and polar components of the total value are included. This shows that there is a small increase in the surface free energy when the surface is solvent wiped, which can be attributed to some of the upper layers of carbon contamination being removed.

3.2 XPS

Figure 2 shows the survey spectra for three stainless steel surfaces treated using different methods. The untreated surfaces comprised predominantly of carbon and oxygen, with a slight indication of iron present. The emergence of the nitrogen peak when the surface is treated may be of interest to this study as the treatment was conducted using pure helium plasma in atmosphere. This implies that there is some mixing of the atmosphere into the plasma, which may then be ionised by collisions with the active species in the plasma plume.

The carbon over layer thickness for the untreated sample is estimated to be ~4.5 nm, which is a considerable amount and is reduced to 0.6 – 0.8 nm for the two plasma treated samples calculated using the composition data shown in Table 5.

Examples of the iron and chromium 2p spectra are shown in Figure 3(a) and (b) respectively. From these it can be seen that the extended treatment time does not affect the state of the iron or chromium. There is a metallic component present in the iron spectrum for each of the treatment durations (707 eV). Compared to the solvent wiped surface, which is lacking this feature. The aforementioned carbon over-layer appears to be attenuating the iron and chromium intensity.

Figure 4 (a) and (b) show the iXPS data for the carbon and oxygen concentration distributions across a treated region. Included is a sample spectrum for each element taken from the centre of the treated region.

4 Discussion

4.1 Surface free energy measurements

Treatment of AISI 316 stainless steel by a pure helium plasma increases the surface free energy from 39mJ m-1 (untreated surface) to 77 mJ m-1, shown in Figure 1. The low starting value is thought to be a result of hydrocarbon contamination from the protective polymer film. An ultrasonic rinse in either isopropyl alcohol or acetone removed some of the contamination but not all of it. This is likely to be the outermost layers of carbon contamination which are generally thought to be loosely bound and non-polar in nature [30].

4.2 XPS

To understand further the surface free energy results, XPS was used to analyse the surface for chemical changes induced by exposure to the plasma. This was initially done by exposing the material to the plasma for five minutes to ensure that any changes would be obvious. As Figure 2 shows, there is a significant reduction in adventitious carbon when comparing the acetone washed sample to the 15 second CAP treated sample and a further reduction for the 5 minute exposure sample. This implies that there is a removal of the carbon contamination layer as opposed to the functionalisation of the hydrocarbon layer.

The survey spectra presented Figure 2 show that there is a limited amount of carbon observed to be present on the metal surface after CAP treatment. This is unavoidable as the formation of a carbon over layer is almost instantaneous when a metal surface is exposed to atmosphere – the driving force being the reduction in surface free energy of the oxidised metal surface by the adsorption of air-borne carbonaceous material. The initial over-layer may increase in thickness with time. This has been minimised by keeping the time between treatment and admittance into the instrument to be less than 2 minutes for each sample.

Importantly, there appears to be a similar level of carbon contamination reduction on the 15 second exposure sample. This implies that the cleaning aspect of the treatment takes place within over a relatively short time.

Further to a large reduction in the carbon content there is a considerable increase in the concentration of oxygen. This may be a result of three processes occurring at the surface.

1. Uncovering of the native oxide layer, will be accompanied by an increase in the iron and chromium peak that can also be seen in the survey spectra in Figure 2.
2. The carbon overlayer itself is being oxidised by the plasma torch, as a result of oxygen from the atmosphere mixes with the plasma plume. This may lead to oxygen being ionised and subsequently available to bond with the carbon contamination

3. As the polar carbon is more firmly attached to the underlying oxide layer, the plasma torch may only remove the uppermost apolar carbon layers, which would reveal more oxygen containing carbon.

The first process can be corroborated on the basis of the O1s binding energy of ca. 530.2, but the second and third processes are difficult to differentiate between as they both involve functionalised carbon at a higher binding energy within the O1s spectrum. The reduction in carbon also indicates that the former process is the dominant feature although the C1s spectrum shows the clear presence of polar adventitious material. Based on the structure of an atmosphere exposed clean surface as shown in Figure 5, following the schema of Castle [30] there may be a limit to the removal of carbon as the polar carbon is more strongly attached to the oxide surface. Therefore, the nonpolar carbon is removed revealing a layer of oxygen containing polar carbon.

To investigate which process occurs, the carbon iXPS data of the treated area is presented as several different maps in Figure 6, which show the intensity of discreet energies within the carbon window. Each has been chosen as they represent different carbon compounds such as C-C (285.0 eV), C-O (286.6 eV) and C=O (288.0 eV).

When viewing the carbon intensity at 285.0 eV (C-C bonds) there is a large void towards the centre of the treated area, shown in Figure 6a and a band of increased intensity some distance away. At 286.5 eV (C-O bonds) there is a ring of increased intensity surrounding the treated region shown in Figure 6b. When the energy is when moved further to 288.0 (O-C=O bonds) [31] the ring moves in closer to the centre of the treated area, Figure 6c.

Figure 6d is a composite image of the previous three images. Each map has been reconstructed using an above average thresholding technique, whereby each pixel intensity is compared to the average intensity of the entire map. If the intensity of a pixel is higher than the average it is considered a value based on Table 6 and if it is lower it is set to 0. The three maps are then summed into a single map, shown in Figure 6d. Binary numbers were used to create a unique value for any summation that may occur, for example a final value of 1 or 2 indicates that only C-C or C-O is the dominant chemical species present. If the value was 3 it shows that there is a mixture of C-C and C-O present at that pixel. The result is a value that will range from 0 - 7.

Figure 6d shows that there is a region of C=O close to the treated area that is not mixed with a significant amount of other carbon species. Surrounding that there is a ring of C=O and C-O containing species and outside of that is a fairly uniform C-C/C-H surface. This, along with the carbon thickness measurements begins to make clear which process is at work.

Figure 7 shows the treated area as a function of carbon overlayer thickness. The reduction in carbon thickness implies that there is a crater carved through the thick adventitious carbon layer present on the native metal. This indicates that there is at least a component of the first process discussed in Section 4.2, which involves some material removal.

The overall outcome of the iXPS does not appear as well defined as this, which implies that there is a second process at work also. This has been alluded to previously. The remaining carbon species are being oxidised by the plasma. Figure 6d shows that this is a possibility.

Further investigation of the treated area was conducted by submerging the treated sample in water and measuring the diameter of the wetted area. A photo of the treated area after submersion is shown below in Figure 8. This shows a wettable diameter of circa 12 mm. The boundary of the drop was then traced and overlaid on a scaled image of the carbon concentration map, this can also be seen in Figure 8 where the red line is the outline of the drop. In this instance, the carbon concentration has been limited in range to 40 – 50% to investigate the boundary between the wetting and non-wetting surface.

From the work conducted on the cold atmospheric plasma treatment of stainless steel, the proposed method of treatment is that of ablation of the carbon contamination covering the metal surface. This occurs over an apparently short period, of the order of several seconds. After that, it is not clear if there is any promotion of the oxide layer when using a pure helium plasma. This is reasonable, as there would be little oxygen being mixed into the plume. Further analysis would be required to confirm this hypothesis such as plasma assisted desorption/ionisation (PADI) spectroscopy of the surface being introduced into the plume. Secondary ion mass spectrometry (SIMS) could also be used to investigate the surface in more detail compared to XPS.

5 Conclusions

Exposure of 316 stainless steel to a cold atmospheric plasma plume reduces the carbon contamination at the surface considerably. This has been done with exposure times from 5 minutes to circa 5 seconds, each of which shows that there is a large reduction in carbon contamination, from 80 at.% to circa 30-40 at.%. This is accompanied by a large increase in surface free energy consistent with an increase in the polar energy calculated.

The increase the polar component of the surface free energy coincides with an increase in oxygen on the surface. This has been shown to be the driving factor for the surface energy differences.

Using a plasma jet with the parameters described in this paper, the treated area is in the region of 10-12 mm diameter. This can be used in further work to optimise the treatment of an area. The difference in treated area and nozzle diameter is down to the gas expanding upon leaving the nozzle.

Acknowledgements

This work was carried out as part of an Engineering Doctorate in Micro and NanoMaterials and Technologies (MiNMaT). DFW gratefully acknowledges support from the ESPRC in providing funding for the MINMaT Centre for doctoral Training (EP/L016788/1) at the University of Surrey.

References

[1] R.A. Difelice, An Investigation of Plasma Pretreatments and Plasma Polymerized Thin Films for Titanium / Polyimide Adhesion, Virginia Polytechnic Institute and State University, 2001.

[2] P. Molitor, V. Barron, T. Young, Surface treatment of titanium for adhesive bonding to polymer composites: A review, Int. J. Adhes. Adhes. 21 (2001) 129–136. doi:10.1016/S0143-7496(00)00044-0.

[3] M. Assefpour-Dezfuly, C. Vlachos, E.H. Andrews, Oxide morphology and adhesive bonding on titanium surfaces, J. Mater. Sci. 19 (1984) 3626–3639. doi:10.1007/BF02396935.

[4] G.W. Critchlow, D.M. Brewis, Review of surface pretreatments for aluminium alloys, Int. J. Adhes. Adhes. 16 (1996) 255–274. doi:10.1016/S0143-7496(96)00014-0.

[5] G.W. Critchlow, Pretreatments for Metal-to-Metal Bonding, Loughborough University, 1997.

[6] D.J. Arrowsmith, A.W. Clifford, Morphology of anodic oxide for adhesive bonding of aluminium, Int. J. Adhes. Adhes. 3 (1983) 193–196.

[7] E. Harscoet, D. Froelich, Use of LCA to evaluate the environmental benefits of substituting chromic acid anodizing (CAA), J. Clean. Prod. 16 (2008) 1294–1305. doi:10.1016/j.jclepro.2007.06.010.

[8] R. Broad, J. French, J. Sauer, CLP new, effective, ecological surface pretreatment for highly durable adhesively bonded metal joints, Int. J. Adhes. Adhes. 19 (1999) 193–198. doi:10.1016/S0143-7496(98)00034-7.

[9] D.F. Williams, M.-L. Abel, E. Grant, J. Hrachova, J.F. Watts, Flame treatment of polypropylene: A study by electron and ion spectroscopies, Int. J. Adhes. Adhes. 63 (2015) 26–33. doi:10.1016/j.ijadhadh.2015.07.009.

[10] A. Baldan, Adhesively-bonded joints and repairs in metallic alloys, polymers and composite materials: Adhesives, adhesion theories and surface pretreatment, J. Mater. Sci. 39 (2004) 1–49. doi:10.1023/B:JMSC.0000007726.58758.e4.

[11] A. Wilson, I. Jones, F. Salamat-Zadeh, J.F. Watts, Laser surface modification of poly(etheretherketone) to enhance surface free energy, wettability and adhesion, Int. J. Adhes. Adhes. 62 (2015) 69–77. doi:10.1016/j.ijadhadh.2015.06.005.

[12] A.J. Harris, B. Vaughan, J.A. Yeomans, P.A. Smith, S.T. Burnage, Surface preparation of silicon carbide for improved adhesive bond strength in armour applications, J. Eur.

Ceram. Soc. 33 (2013) 2925–2934. doi:10.1016/j.jeurceramsoc.2013.05.026.

[13] H. Conrads, M. Schmidt, Plasma generation and plasma sources, Plasma Sources Sci. Technol. Plasma Sources Sci. Technol. 9 (2000) 441–441.

[14] A. Carrado, O. Sokolova, B. Donnio, H. Palkowski, Influence of Corona Treatment on Adhesion and Mechanical Properties in Metal/Polymer/Metal Systems, J. Appl. Polym. Sci. 120 (2011) 3709–3715. doi:10.1002/app.

[15] T.S. Williams, H. Yu, R.F. Hicks, Atmospheric pressure plasma activation as a surface pre-treatment for the adhesive bonding of aluminum 2024, J. Adhes. Sci. Technol. 28 (2014) 653–674. doi:10.1080/01694243.2013.859646.

[16] Y.S. Seo, A. -a. H. Mohamed, K.C. Woo, H.W. Lee, J.K. Lee, K.T. Kim, Comparative Studies of Atmospheric Pressure Plasma Characteristics Between He and Ar Working Gases for Sterilization, IEEE Trans. Plasma Sci. 38 (2010) 1–9.

[17] M.C. Kim, D.K. Song, H.S. Shin, S.-H. Baeg, G.S. Kim, J.-H. Boo, J.G. Han, S.H. Yang, Surface modification for hydrophilic property of stainless steel treated by atmospheric-pressure plasma jet, Surf. Coatings Technol. 171 (2002) 312–316. doi:10.1016/S0257-8972(03)00292-5.

[18] John R Roth, Peter P Tsai, Method and apparatus for glow discharge plasma treatment of polymer materials at atmospheric pressure, 5456972, 1996.

[19] Ö. Birer, Reactivity zones around an atmospheric pressure plasma jet, in: Appl. Surf. Sci., 2015: pp. 420–428. doi:10.1016/j.apsusc.2015.04.100.

[20] V. Cristaudo, S. Collette, C. Poleunis, F. Reniers, A. Delcorte, Surface Analysis and Ultra-Shallow Molecular Depth-Profiling of Polyethylene Treated by an Atmospheric Ar-D<inf>2</inf>O Post-Discharge, Plasma Process. Polym. (2015). doi:10.1002/ppap.201400248.

[21] a Schutze, J.Y. Jeong, S.E. Babayan, J. Park, G.S. Selwyn, R.F. Hicks, The atmospheric-pressure plasma jet: a review and comparison to other plasma sources, Plasma Sci. IEEE Trans. 26 (1998) 1685–1694. doi:10.1109/27.747887.

[22] R.F. Hicks, H.W. Herrmann, R.F. Hirsch, K.-C. Chang, Atmospheric-Pressure Plasma Cleaning of Contaminated Surfaces, (n.d.).

[23] C. Qian, Z. Fang, J. Yang, M. Kang, Investigation on atmospheric pressure plasma jet array in ar, IEEE Trans. Plasma Sci. 42 (2014) 2438–2439. doi:10.1109/TPS.2014.2324577.

[24] I. Motrescu, M. Nagatsu, Nanocapillary Atmospheric Pressure Plasma Jet: A Tool for

Ultrafine Maskless Surface Modification at Atmospheric Pressure, ACS Appl. Mater. Interfaces. (2016). doi:10.1021/acsami.6b02483.

[25] T. Scott, T.S. Williams, Surface Modification by Atmospheric Pressure Plasma for Improved Bonding A dissertation submitted in partial satisfaction of the by, (2013).

[26] C. Tendero, C. Tixier, P. Tristant, J. Desmaison, P. Leprince, Atmospheric pressure plasmas: A review, Spectrochim. Acta Part B At. Spectrosc. 61 (2006) 2–30. doi:10.1016/j.sab.2005.10.003.

[27] D. Rymuszka, K. Terpiłowski, L. Hołysz, Influence of volume drop on surface free energy of glass, 2013. doi:10.2478/umcschem-2013-0010.

[28] F.M. Fowkes, Attractive forces at interfaces, Ind. Eng. Chem. 56 (1964) 40–52. doi:10.1021/ie50660a008.

[29] G.C. Smith, Evaluation of a simple correction for the hydrocarbon contamination layer in quantitative surface analysis by XPS, J. Electron Spectros. Relat. Phenomena. 148 (2005) 21–28. doi:10.1016/j.elspec.2005.02.004.

[30] J.E. Castle, The Composition of Metal Surfaces After Atmospheric Exposure: An Historical Perspective, J. Adhes. 84 (2008) 368–388. doi:10.1080/00218460802004477.

[31] D. Briggs, Surface Analysis of Polymers by XPS and Static SIMS, Cambridge University Press, 1998.

Figure Captions

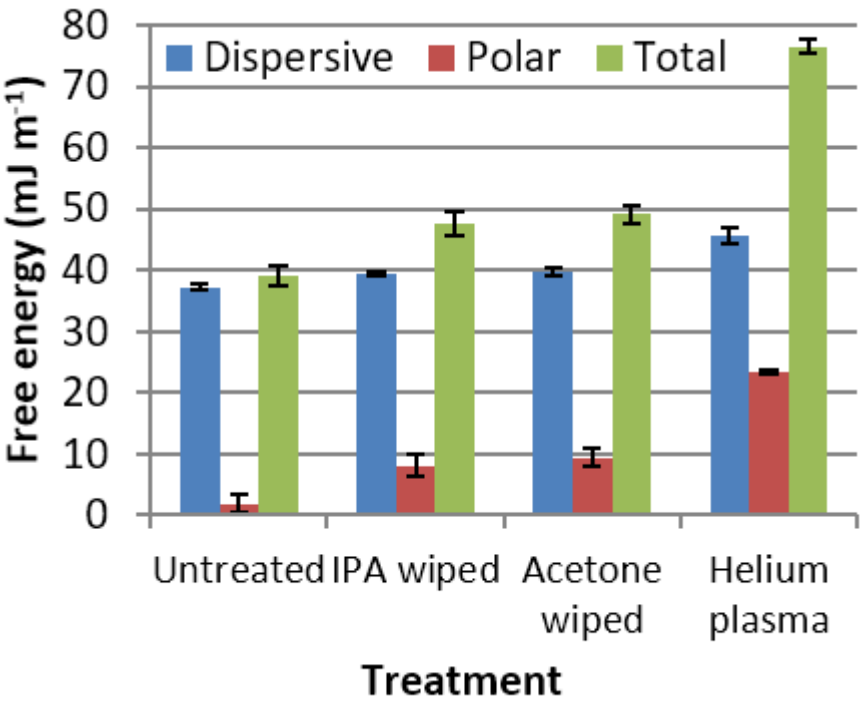

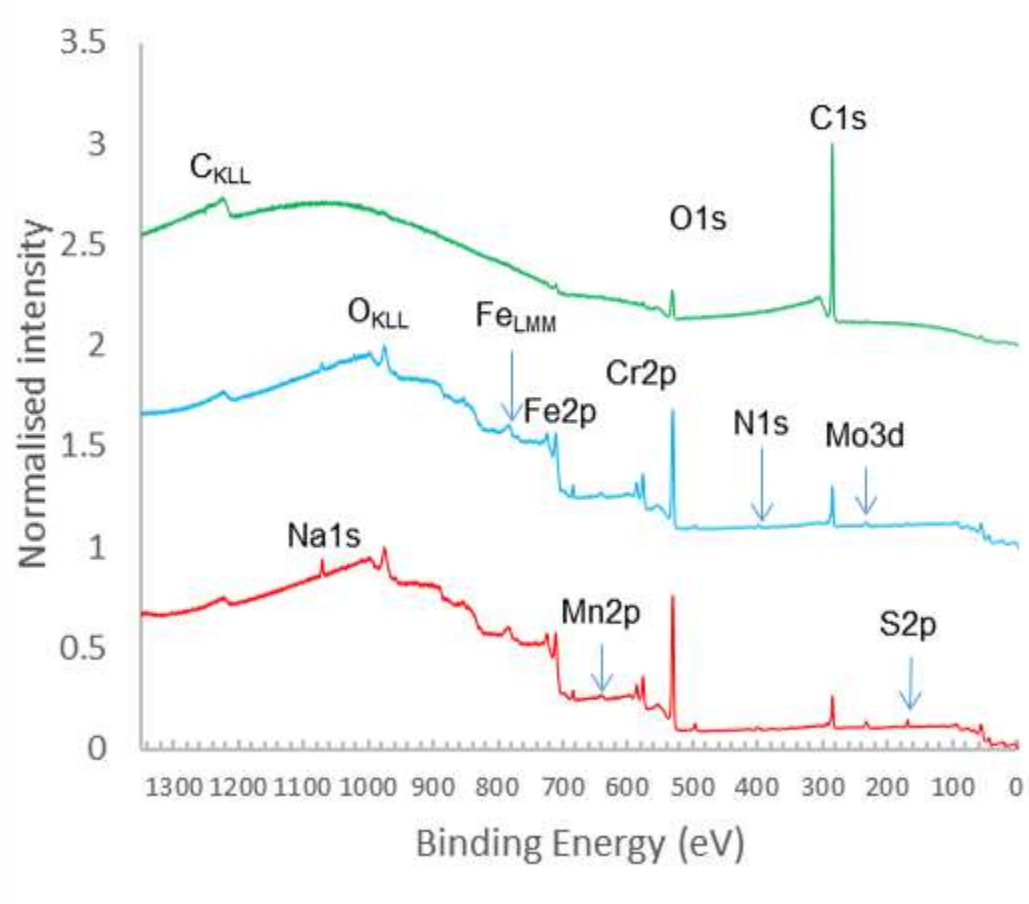

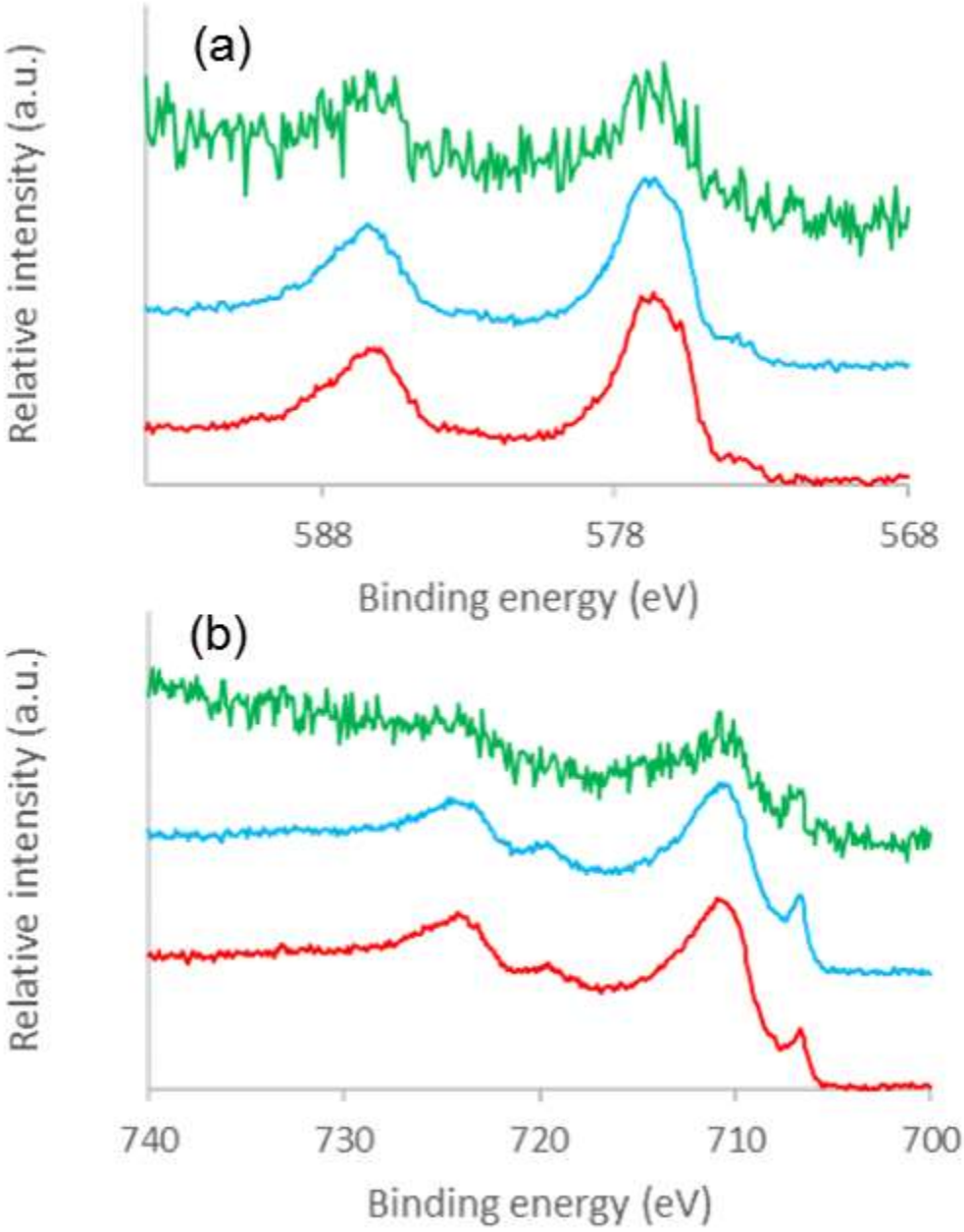

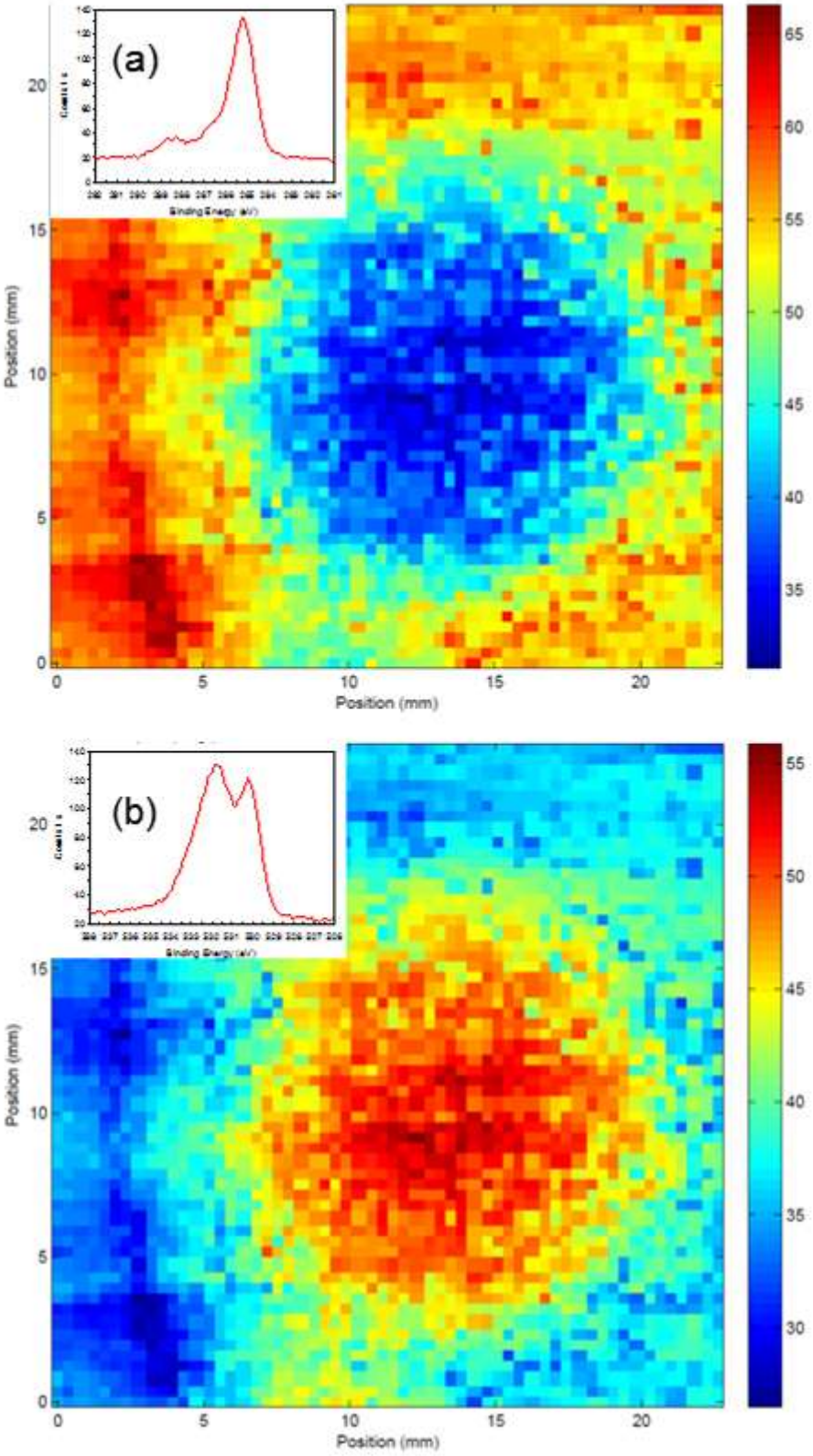

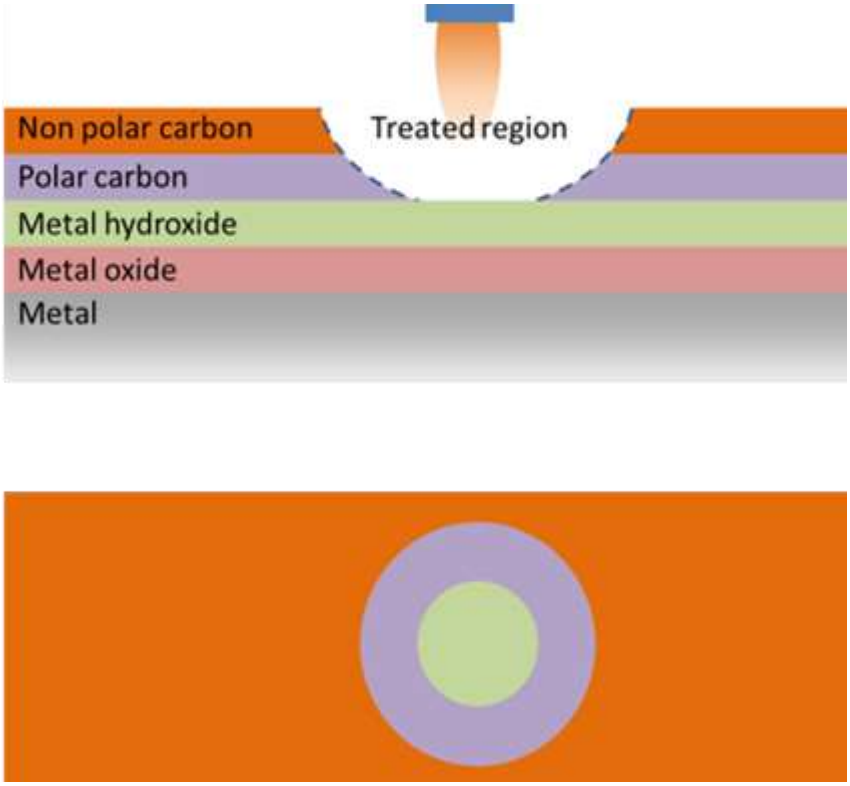

Figure 6 - XPS of treated area using individual peak intensity from carbon scan shown in Figure 4. (a) 285.0 eV, (b) 286.5 eV and (c) 288.0 eV. (d) map of the distribution using codes from 20

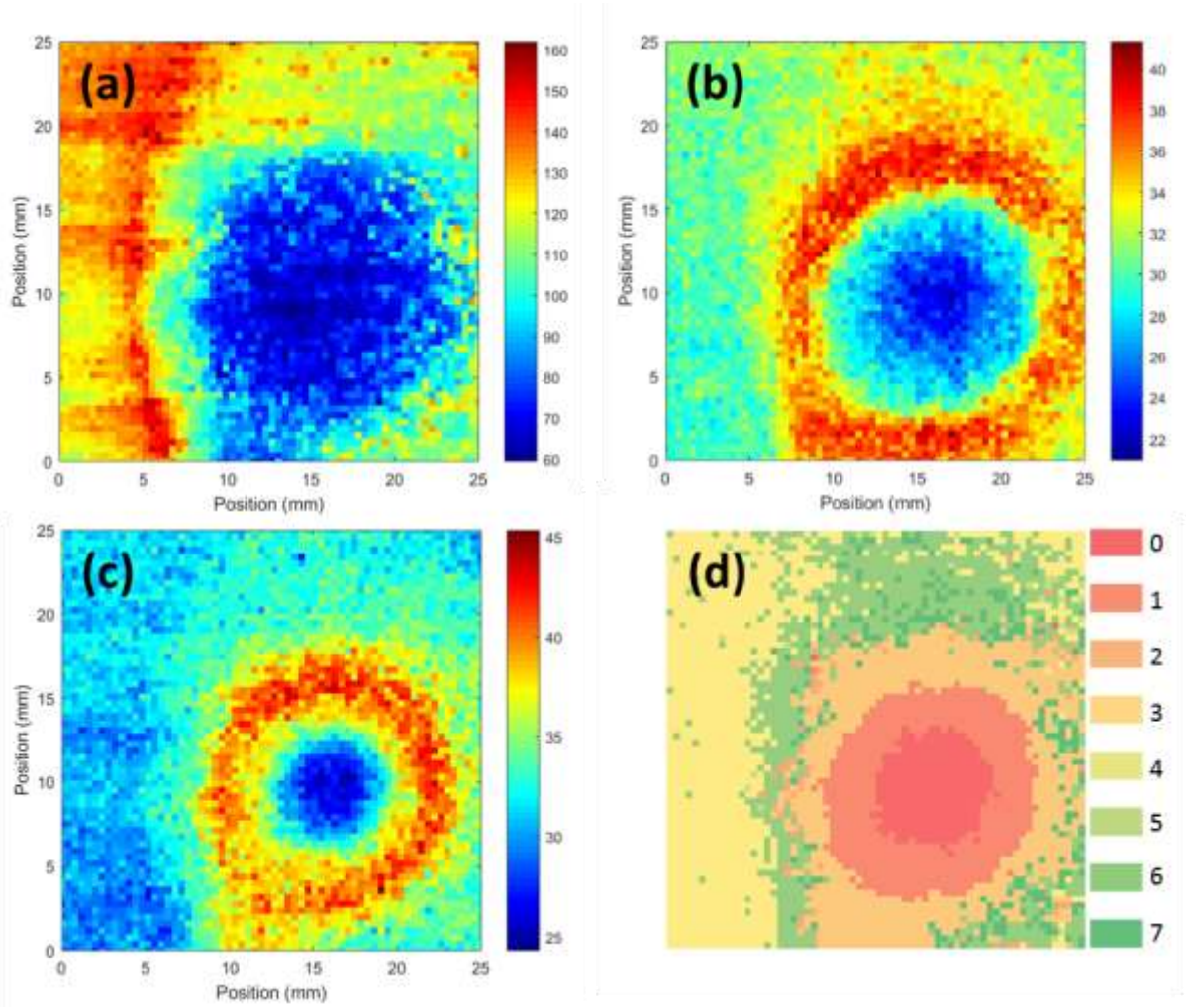

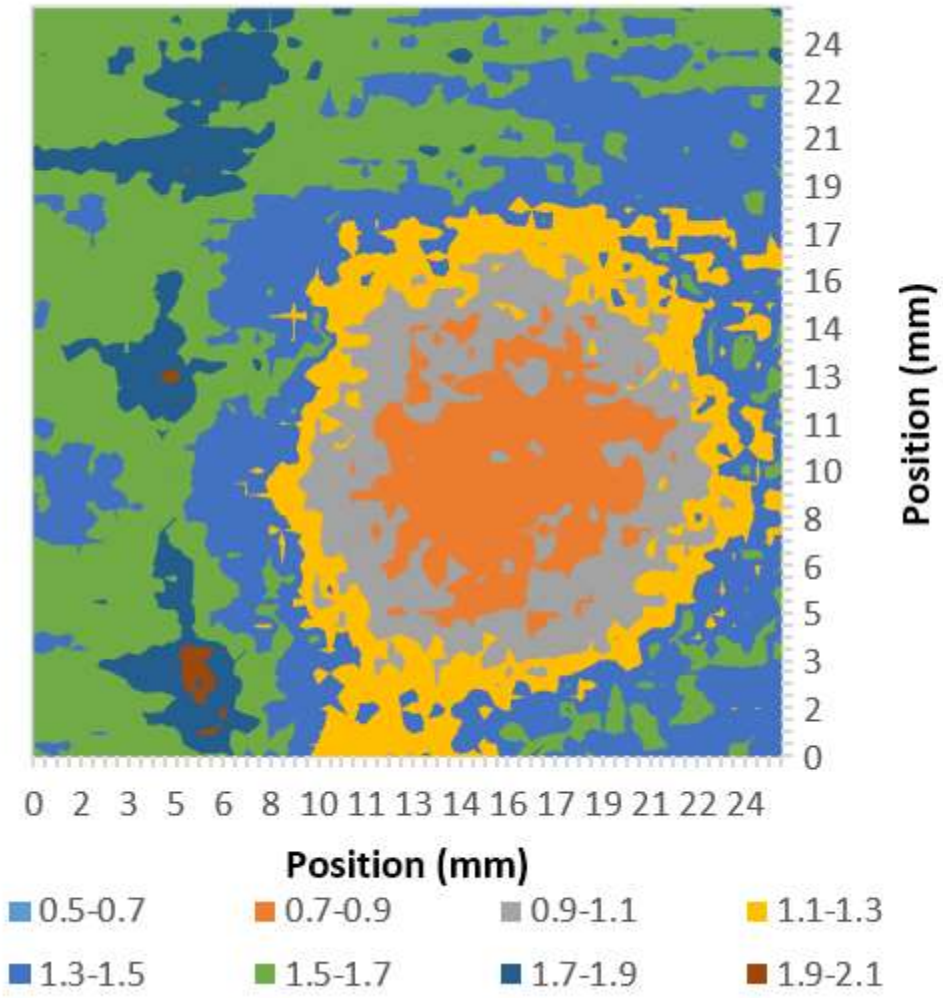

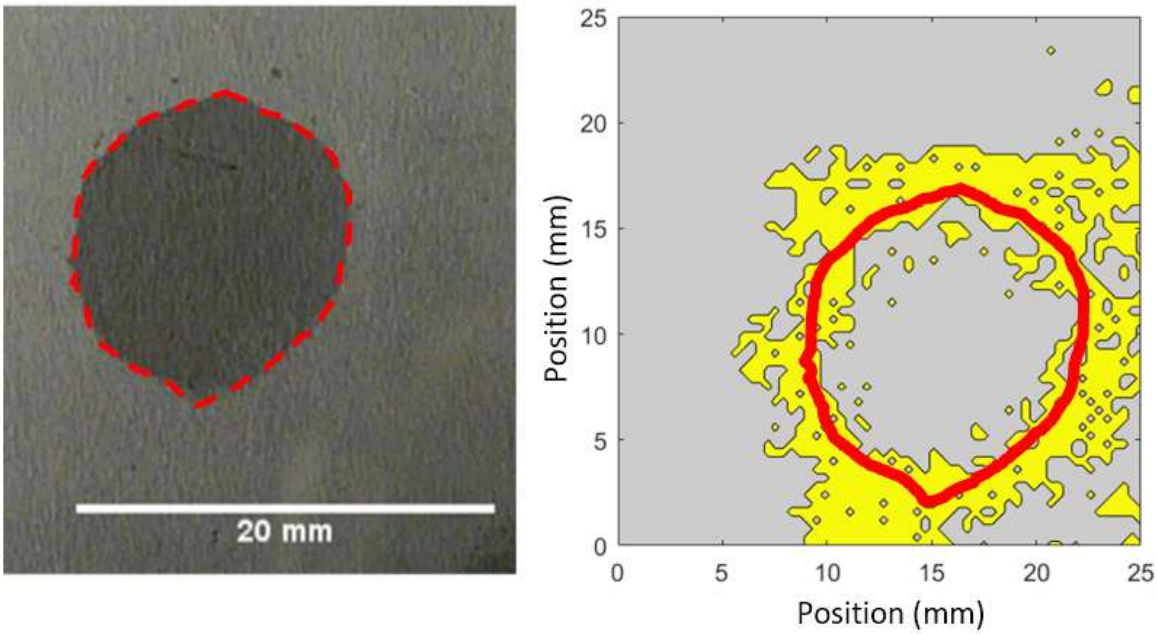

Tables

Table 1 Nominal composition and composition in weight% of 316 stainless steel

	Fe	Cr	Ni	C	Mo	Mn	Si	P	S
AISI 316 spec	Bal	16-18	10-14	<0.08	2-3	<2	<1	<0.045	<0.03
Test samples	Bal	16.5	10.2	0.02	2.00	1.40	0.50	0.02	0.003

Table 2 gas combinations possible for this investigation

Primary gas	Secondary gas
Helium	Oxygen (argon only)
Argon	Air
	Nitrogen (helium only)
	Water vapour

Table 3 Parameter used for the plasma treatment

Parameter	Value
Stand off distance (mm)	5
Total indicated inlet gas flow rate (l min^{-1})	8
Torch Velocity (mm min^{-1})	150
Input gas	Helium

Table 4 Snapshot analysis settings

Element	Analysis window (eV)	Pass energy
Carbon	281 – 292	116.9
Chromium	568 – 594	276.3
Iron	700 – 722	233.8
Nitrogen	390 – 405	180.7
Oxygen	526 – 538	127.5

Table 5 Composition data for the samples shown in Figure 2

	Carbon	Chromium	Iron	Molybdenum	Nitrogen	Oxygen
As received	79.5	0.9	1.3		1.9	16.4
15 second treatment	39.5	6.4	9.5	0.4	2.5	41.8
5 minute treatment	28.8	4.8	10.3	0.9	2.2	53.0

Table 6 Values given for each carbon species for Figure 8(d)

Carbon species	Value
C-C	4
C-O	2
C=O	1